Virtual Element Method: An overview of formulations

Tiago F. Moherdaui[1], Alfredo Gay Neto[1]

[1]*Dept. of Structural and Geotechnical Engineering, University of São Paulo*
Av. Prof. Almeida Prado, 83, 05508-070, São Paulo, Brazil
tiago.moherdaui@usp.br, alfredo.gay@usp.br

Abstract. The virtual element method has been around for about a decade, and it has been through a lot of development during this period. The method generalizes the finite element method for polytopal elements, while retaining optimal convergence properties. This is achieved mainly by implicitly defined function spaces and the use of polynomial projections. This work presents an overview of the development of the method as formulated for elliptic problems in two and three dimensions, here represented by Poisson's equations. The formulations covered are: its original formulation, the modified formulation enabling three-dimensional elements, the Serendipity formulation, and one of the formulations for self-stabilized elements.

Keywords: Virtual element method

1 Introduction

Over ten years have passed since the introduction of its abstract framework in Beirão da Veiga et al. [1]. In this time, the method has been developed in many different ways, such as solution regularity (da Veiga and Manzini [2]), discretization of vectors spaces (da Veiga et al. [3]), mixed formulations (Brezzi et al. [4]), etc. The method has also found some applications in which it stands out such as: topology optimization (Chi et al. [5]), where the use of polytope elements avoids some of the common problems of simplices and quads; and fields where the discrete spaces are required to form exact Stokes or de Rham complexes (e.g., da Veiga et al. [6]).

This work presents four formulations of virtual elements for elliptical problems (represented by Poisson's equations), with focus on the definitions of the function space, the different projectors and how they are used. The rest of the paper is outlined as follows. Poisson's equations are briefly presented in Section 2, as the toy problem for which the formulations are discussed. In sequence come the presentation of the formulations in Section 3 and subsections therein. Followed by a simple numerical example in Section 4 and the conclusions in Section 5.

2 Poisson's Equations

Poisson's equations describe a linear elliptic problem of determining a function by its Laplacian and boundary conditions. The problem formulation consists in finding the solution $u : \Omega \to \mathbb{R}$ defined over a domain $\Omega \subset \mathbb{R}^d$ with spatial dimensions $d = 2, 3$, with Laplacian prescribed as the opposite of a function $g : \Omega \to \mathbb{R}$. This solution has also to satisfy Dirichlet ($u = \bar{u}$ in Γ_D) and Neumann ($\nabla u \cdot \mathbf{n} = f$ in Γ_N, for some $f : \Gamma_N \to \mathbb{R}$, $\mathbf{n}$ being the outward unit normal vector to Γ_N) boundary conditions, with $\partial\Omega = \Gamma_D \cup \Gamma_N,\ \Gamma_D \cap \Gamma_N = \emptyset$; as in eq. (1).

$$\begin{cases} -\Delta u = g & \text{in } \Omega \\ u = \bar{u} & \text{on } \Gamma_D \\ \nabla u \cdot \mathbf{n} = f & \text{on } \Gamma_N \end{cases}, \tag{1}$$

and with weak formulation consisting in: Find $u \in H^1(\Omega)$ such that for all $\delta u \in H^1_0(\Omega)$, eq. (2) holds.

$$\begin{cases} \int_\Omega \nabla u \cdot \nabla \delta u \, d\Omega = \int_\Omega g \delta u \, d\Omega + \int_{\Gamma_N} f \delta u \, d\sigma \\ u = \bar{u} \text{ on } \Gamma_D \end{cases}. \tag{2}$$

With $H_0^1(\Omega)$ being the restriction of $H^1(\Omega)$ satisfying homogeneous Dirichlet boundary condition.

3 Virtual Element Formulations

The following sections will present the four chosen virtual element method formulations in chronological order of their publication, starting with a preliminaries section to introduce some notation and concepts.

Let the problem domain Ω be partitioned into a set of polytopal (polygons/polyhedra) subdomains $\mathcal{T}_h$. The notational convention is that when an affirmation is valid for general polytopes, they will be referred to as E, by P when it only applies to polyhedra, and F when exclusive to polygons. For all $E \in \mathcal{T}_h$ the maximum distance between two points is given by h_E and called its diameter, its centroid is $\mathbf{x}_E$, and $h = \max_{E \in \mathcal{T}_h} h_E$ is referred to as the mesh diameter. A polygon F is characterised by its n_V vertices, has $n_E = n_V$ edges, and its area is $|F|$. A polyhedron P has n_V vertices, n_E edges, n_F faces and its volume is $|P|$. These are shown in Fig. 1.

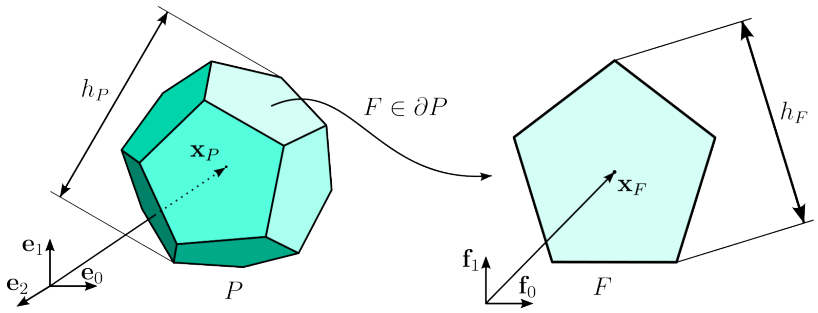

Figure 1. Generic polyhedron P and polygonal face F.

Recall the formal definition of a finite element as a triplet (E, V^h, Σ), given in Ciarlet [7], where $E \subset \mathbb{R}^d$ is the domain of the element, V^h is a function space defined over E, and $\Sigma = \{dof_i\}$ is a basis of the dual space of V^h, also known as the set of degrees of freedom. In the same reference one also finds that the convergence rate for the element is associated with its function space V^h containing a full polynomial space. This is fundamental for virtual element spaces as they are designed to contain a full polynomial subspace, thus the superscript h will be dropped as it is always implied, and a subscript k will be adopted for virtual element function spaces to denote the order up to which the full polynomial subspace is contained $V_k(E) \supseteq \mathcal{P}_k(E)$.

Projectors onto polynomial spaces play an important role in virtual element formulations. Let $\mathcal{P}_k(E)$ denote the space of polynomials of order up to k in d variables ($E \subset \mathcal{R}^d$). For the purpose of this exposition, projectors will take a function from the element space (or its derivative) to the closest polynomial according to some notion of distance used to ensure orthogonality. An example to illustrate the notation is the L^2 projector $\Pi_k^0 : V_k \to \mathcal{P}_k$, which uses the L^2 inner product to define the orthogonality condition in eq. (3), where I is the identity operator.

$$\int_E (I - \Pi_k^0) v p d\mathbf{x} = 0, \ \forall p \in \mathcal{P}_k(E), \ v \in V_k(E). \tag{3}$$

By choosing a basis $\{\phi_i\}$ for $V_k(E)$ and $\mathcal{M}_k = \{m_\alpha\}$ being the scaled monomial basis for $\mathcal{P}_k(E)$, one can find a matrix representation for the projector as shown in eq. (4).

$$\begin{aligned} \mathbf{\Pi}_k^0 &= \mathbf{G}^{-1}\mathbf{B}; \\ G_{\alpha,\beta} &= \int_E m_\alpha m_\beta d\mathbf{x}; \\ B_{\alpha,i} &= \int_E m_\alpha \phi_i d\mathbf{x}. \end{aligned} \tag{4}$$

This is the general form of all projectors, the difference being that sometimes $\mathbf{B} = \mathbf{B}^\nabla - \mathbf{B}^\Delta$ is split into boundary ($\mathbf{B}^\nabla$) and domain ($\mathbf{B}^\Delta$) integrals when integration by parts is used. In general, latin indices (e.g., $i, \ j$) refer to the basis functions of the virtual element space and range from 1 to n_{DOF} (total number of degrees of freedom) unless otherwise stated, and greek indices (e.g., $\alpha, \ \beta$) refer to elements of the scaled monomial basis

of the codomain of the projection, their range is assumed to be from 1 to the dimension of the codomain unless stated otherwise. The scaled monomials are common in the VEM literature (see da Veiga et al. [8] for more detail), and are a basis centered on the element centroid and where each coordinate is scaled by the inverse of the element diameter, i.e., coinciding with the canonical basis on a polytope centered at the origin and scaled to have unit diameter.

To conclude this section, one more preliminary concept to be introduced is the auxiliary boundary space $\mathcal{B}_k(\partial F)$ which is common to all formulations.

$$\mathcal{B}_k(\partial F) := \left\{ v \in C^0(\partial F) : v|_e \in \mathcal{P}_k(e) \ \forall \text{ edge } e \in \partial F \right\}. \tag{5}$$

3.1 Original Formulation

The space presented in eq. (6) is the one introduced in Beirão da Veiga et al. [1], it is denoted with superscript O standing for original. One can verify that this space contains $\mathcal{P}_k(F)$ as a subspace.

$$V_k^O(F) := \left\{ v \in H^1(F) \cap B_k(\partial F) : \Delta v \in \mathcal{P}_{k-2}(F) \right\}. \tag{6}$$

The degrees of freedom for a function v in this formulation are as follow.

- The values at the vertices of F - $v(\mathbf{x}_V)$.
- The values at $k-1$ points on each edge - $v(\mathbf{x}_e)$.
- The internal moment with respect to each monomial in $\mathcal{M}_{k-2}$ as in eq. (7).

$$\frac{1}{|F|} \int_F v m_\alpha d\mathbf{x} \tag{7}$$

This formulation relies on a projector based on the left-hand side of eq. (2), $\Pi_k^\nabla : V_k^O \to \mathcal{P}_k$, which is based on the orthogonality condition in eq. (8), to compute the gradients in the weak formulation.

$$\int_F \nabla(I - \Pi_k^\nabla)v \cdot \nabla p d\mathbf{x} = 0, \ \forall p \in \mathcal{P}_k(F), \ \forall v \in V_k^O(F). \tag{8}$$

The matrices analogue to those in eq. (4) for this projector are shown in eq. (9), with the observation that the constant component is supplied by another projector (see da Veiga et al. [8] for more detail).

$$\begin{aligned} G_{\alpha,\beta} &= \int_F \nabla m_\alpha \cdot \nabla m_\beta d\mathbf{x}; \\ B^\nabla_{\alpha,i} &= \int_{\partial F} (\nabla m_\alpha \cdot \mathbf{n}) \phi_i d\sigma \\ B^\Delta_{\alpha,i} &= \int_F \phi_i \Delta m_\alpha d\mathbf{x} \end{aligned} \tag{9}$$

These are computable from the degrees of freedom of the element. $\mathbf{G}$ consists of polynomial integrals; $\mathbf{B}^\nabla$ is the same, as $\phi_i|_{\partial F} \in \mathcal{B}_k$ implies these functions are polynomials at each edge by definition; and $\mathbf{B}^\Delta$ is obtained with the definition of the internal moment degrees of freedom in eq. (7), scaled by $|F|$.

Furthermore, the L^2 projector shown in eq. (3) can only be computed up to order $k-2$, as it is limited by the available internal moment degrees of freedom. This projector is used to approximate the load term in eq. (2), i.e., the integral with g, and it is shown that Π^0_{k-2} is sufficient for this purpose (see da Veiga et al. [8]).

The major caveat of this formulation arises when one tries to extend it to three-dimensional elements. The equivalent formulation would be the one shown in eq. (10).

$$V_k^O(P) := \left\{ v \in H^1(P) : v|_F \in V_k^O(F) \forall F \in \partial P, \ \Delta v \in \mathcal{P}_{k-2}(P) \right\}. \tag{10}$$

The problem comes when computing Π_k^∇, as $\mathbf{B}^\nabla$ would require moments of order $k-1$ for the functions in the faces. This could be solved by requiring faces to have internal moment degrees of freedom up to order $k-1$, however, a better way was found, as presented in the following section.

3.2 Modified Formulation

This formulation was motivated by the restrictions to the L^2 projection and 3D formulation presented at the end of the last section, and published in Ahmad et al. [9]. It consists in introducing a wider auxiliary space $\tilde{V}_k^M$ and then later restricting it to a subspace that satisfies a desirable property, much like one would find a specific level-set curve. The spaces for both two and three dimensions are presented in eq. (11).

$$\begin{aligned}
\tilde{V}_k^M(F) &:= \left\{ v \in H^1(F) \cap B_k(\partial F) : \Delta v \in \mathcal{P}_k(F) \right\}; \\
V_k^M(F) &:= \left\{ v \in \tilde{V}_k^M(F) : \int_F v p d\mathbf{x} = \int_F \Pi_k^\nabla v p d\mathbf{x} \forall p \in \mathcal{P}_k / \mathcal{P}_{k-2} \right\}; \\
\tilde{V}_k^M(P) &:= \left\{ v \in H^1(P) : v|_F \in V_k^M(F) \forall F \in \partial P,\ \Delta v \in \mathcal{P}_k(P) \right\}; \\
V_k^M(P) &:= \left\{ v \in \tilde{V}_k^M(P) : \int_P v p d\mathbf{x} = \int_P \Pi_k^\nabla v p d\mathbf{x} \forall p \in \mathcal{P}_k / \mathcal{P}_{k-2} \right\}.
\end{aligned} \tag{11}$$

The auxiliary space $\tilde{V}_k^M(E)$ is wider than $V_k^O(E)$, as its restriction on the Laplacian of the function is more relaxed. To determine a function in this space, additional internal moment degrees of freedom would be required, i.e., the moments with respect to monomials up to order k. However, the space $V_k^M(E)$ is a restriction to those functions whose moments of orders higher than $k-2$ coincide with those of the Π_k^∇ projection, effectively fixing these additional degrees of freedom which can be used to compute Π_k^0 and enable the three dimensional version of the method. In the authors' words, what happens is that $V_k^M(E)$ prescribes these additional internal moment using Π_k^∇. This is all done without requiring any change in the degrees of freedom previously defined.

With this formulation, one can also compute $\Pi_{k-1}^0 \nabla : V_k^M \to (\mathcal{P}_{k-1})^d$, i.e., a projector that finds the vector of polynomials that best approximates the gradient of the function its projecting. This is an alternative approach to computing the gradient for the weak formulation, i.e., $\Pi_{k-1}^0 \nabla v$ instead of $\nabla \Pi_k^\nabla v$. The L^2 projection of the gradient is shown to be better for some nonlinear problems, see da Veiga et al. [10]. However, as one already has to compute the more complicated Π_k^∇ to be able to prescribe the additional internal moments, it seems more efficient to use it to compute the weak formulation when possible.

3.3 Serendipity Formulation

The motivation for the Serendipity formulation (da Veiga et al. [11]) is the reduction of the number of internal degrees of freedom. To see how some degrees of freedom can be unnecessary, one can look at a quadratic triangular element: the finite element has the full polynomial space $\mathcal{P}_2$ as function space with $\dim \mathcal{P}_2 = 6$ degrees of freedom, all of them being boundary DOFs. The virtual element of same shape and order would have 7 degrees of freedom, the same boundary ones plus one internal moment. Considering that the core idea behind the virtual element method is to use the polynomial projection, this 7th degree of freedom seems redundant.

The core idea behind this formulation is that the boundary degrees of freedom should be preserved, as they ensure continuity of the solution, and only the internal moment DOFs strictly required to identify a polynomial of the desired order are kept. These internal DOFs are required when traceless polynomials are involved, i.e., when the order of the element is higher than or equal to the degree of the bubble function, which is the number of unique support hyperplanes η_E (lines in 2D and planes in 3D) required to fully identify the boundary. The remaining internal DOFs would include this bubble function as a weight in their definition, with some caveats regarding concavities more on which can be found in the original work.

Therefore, it is possible to define a smaller set of the degrees of freedom originally defined in 3.1 that are required to compute a least squares projection onto polynomials Π_k^S, which is in turn used to prescribe all the necessary internal moments. Thus, comes the formulation for the Serendipity virtual element function space presented in eq. (12), with the observation that $\mathcal{P}_k = \{0\}$ for $k < 0$.

$$V_k^S(E) := \left\{ v \in \tilde{V}_k^M(E) : \int_F v p d\mathbf{x} = \int_F \Pi_k^S v p d\mathbf{x} \forall p \in \mathcal{P}_k / \mathcal{P}_{k-\eta_E} \right\}. \tag{12}$$

The reduction in total number of degrees of freedom of the mesh is notable, especially in the three-dimensional case, where internal degrees of freedom in faces represent a considerable fraction of the total. The least squares projection is simple to compute, and it also makes the approach of using the L^2 projection of the gradient ($\Pi_{k-1}^0 \nabla$) instead of the gradient of the original projector ($\nabla \Pi_k^\nabla$) in the weak formulation.

3.4 Stabilization Free Formulation

The formulation presented here for self-stabilized virtual elements is equivalent to the one in Chen and Sukumar [12], which originated in D'Altri et al. [13]. The main idea consists in using an L^2 projection of the gradient onto a polynomial space with order $l > k-1$, which would provide the missing rank to stabilize the element. The choice of l is not fully determined, but expressions have been provided in Chen and Sukumar [12] for the 2D case, and the 3D case has been discussed for $k = 1$ in Xu and Wriggers [14]. To be able to compute this higher order projection, internal moments have to be known with respect to higher order monomials, which would increase the number of internal degrees of freedom. This is offset by the use of the Serendipity formulation, thus, depending on the element's geometry, one can get the self-stabilized version without need for additional degrees of freedom than those of the boundary. Denoting element order k and gradient projection order l, the space definition is in eq. (13).

$$\begin{aligned}
\tilde{V}_{k,l}^{SF}(F) &:= \left\{ v \in H^1(F) \cap B_k(\partial F) : \Delta v \in \mathcal{P}_{l-1}(F) \right\}; \\
\tilde{V}_{k,l}^{SF}(P) &:= \left\{ v \in H^1(P) : v|_F \in V_{k,l+1}^{SF}(F) \forall F \in \partial P,\ \Delta v \in \mathcal{P}_{l-1}(P) \right\}; \\
V_{k,l}^{SF}(E) &:= \left\{ v \in \tilde{V}_k^{SF}(E) : \int_E vpd\mathbf{x} = \int_E \Pi_k^S vpd\mathbf{x} \forall p \in \mathcal{P}_{l-1}/\mathcal{P}_{k-\eta_E} \right\};
\end{aligned} \tag{13}$$

With this formulation, one can make the most of the internal moments available from the serendipity formulation, using them to supply the stabilization term. There is still much to explore with this formulation, especially regarding the determination of the order l, which is still conjectured for the 2D case and its discussion for 3D is restricted to linear elements ($k = 1$). The reliable way to obtain this parameter correctly is to perform eigenvalue analyses for different l's for each polyhedron and find the smallest without spurious zero eigenvalues.

4 Numerical Example

In this section a brief example is shown with concrete applications of three of these four formulations, the original being omitted as it coincides with the modified one in practice. The example is restricted to the 2D setting, and consists in a convergence study using linear and quadratic elements for three polygonal meshes (M1-M3) generated by the Voronoi dual of triangulations of the unit square centred at the origin (Fig. 2).

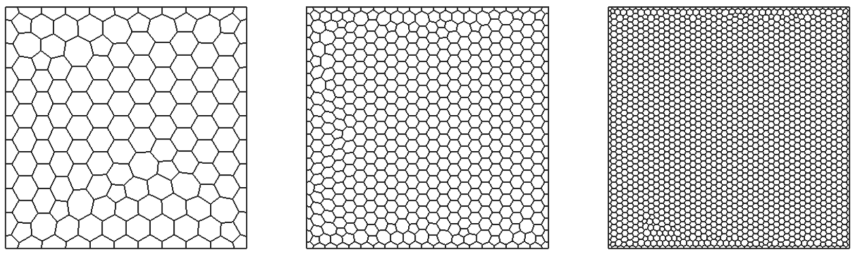

Figure 2. Meshes M1, M2 and M3.

For this study, a third order polynomial solution $u = 3(x^3+y^3+xy)$ (Fig. 3) is chosen. The L^2 and H^1 errors are computed, the former by using Π_k^0 and the latter with the gradient projection as described in each formulation.

For each formulation and order, an exponential curve $e = Ch^p$ is fitted for the computed errors (e) in terms of the mesh size (h). The resulting parameters C and p are shown in Tables 1 and 2 along with the raw errors and the R^2 of the fitting. The same results are shown in the usual graphical form of convergence curves in Fig. 4. One can see that the optimal convergence rates are preserved for all formulations with good adherence of the results to the fitted curves. Regarding the stabilization stiffness matrix when required, the approach employed was the one known as "dofi-dofi" in the recent VEM literature, as presented in da Veiga et al. [8] with the projector Π_k^∇ for the Modified formulation, and an analogue version with Π_k^S is used for the Serendipity one.

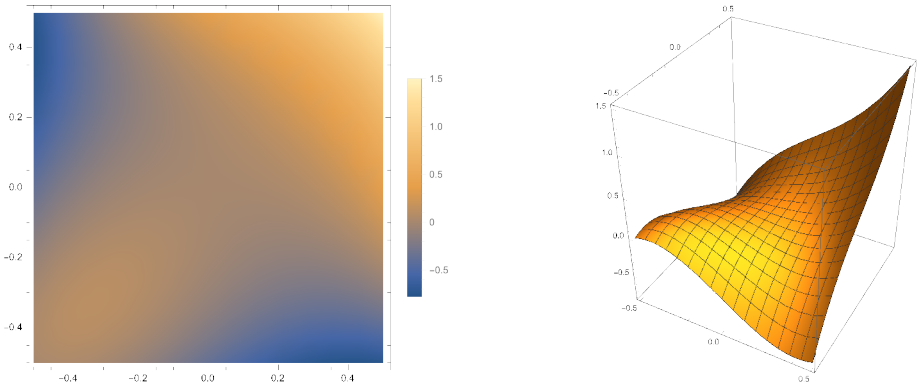

Figure 3. Chosen solution as a colormap (a) and 3D plot (b).

Table 1. L^2-error and fitting parameters.

L^2-Error	M1	M2	M3	C	p	R^2
V_1^M	3.63E-03	1.04E-03	2.66E-04	0.16	1.89	1.00
V_1^S	3.63E-03	1.04E-03	2.66E-04	0.16	1.88	1.00
$V_{1,l}^{SF}$	3.60E-03	1.03E-03	2.63E-04	0.16	1.89	1.00
V_2^M	1.03E-04	1.38E-05	1.73E-06	0.04	2.94	1.00
V_2^S	1.13E-04	1.52E-05	1.91E-06	0.04	2.94	1.00
$V_{2,l}^{SF}$	1.12E-04	1.51E-05	1.91E-06	0.04	2.93	1.00

Table 2. H^1-error and fitting parameters.

H^1-Error	M1	M2	M3	C	p	R^2
V_1^M	2.00E-01	1.08E-01	5.50E-02	1.30	0.93	1.00
V_1^S	2.00E-01	1.08E-01	5.50E-02	1.30	0.93	1.00
$V_{1,l}^{SF}$	1.28E-01	6.89E-02	3.49E-02	0.84	0.93	1.00
V_2^M	8.30E-03	2.19E-03	5.54E-04	0.42	1.95	1.00
V_2^S	8.29E-03	2.19E-03	5.54E-04	0.42	1.95	1.00
$V_{2,l}^{SF}$	7.96E-03	2.07E-03	5.20E-04	0.41	1.97	1.00

5 Conclusions

Ever since its first introduction the virtual element method has been through significant development, and this overview of some of its formulations provides a better understanding on its workings and the motives behind each change it has undergone. To complement the theoretical exposition, a convergence study is provided for the presented formulations in the setting of a 2D Poisson problem, showing that all of them recover the optimal convergence rates for both $k = 1$ and $k = 2$.

Acknowledgements. This work was financed in part by the Coordenação de Aperfeiçoamento de Pessoal de Nível Superior - Brasil (CAPES) - Finance Code 001, and supported by Vale S.A. through the Wheel-Rail Chair project. The second author acknowledges CNPq (Conselho Nacional de Desenvolvimento Científico e Tecnológico), Brazil for the financial support under the research grant 304321/2021-4.

Authorship statement. The authors hereby confirm that they are the sole liable persons responsible for the au-

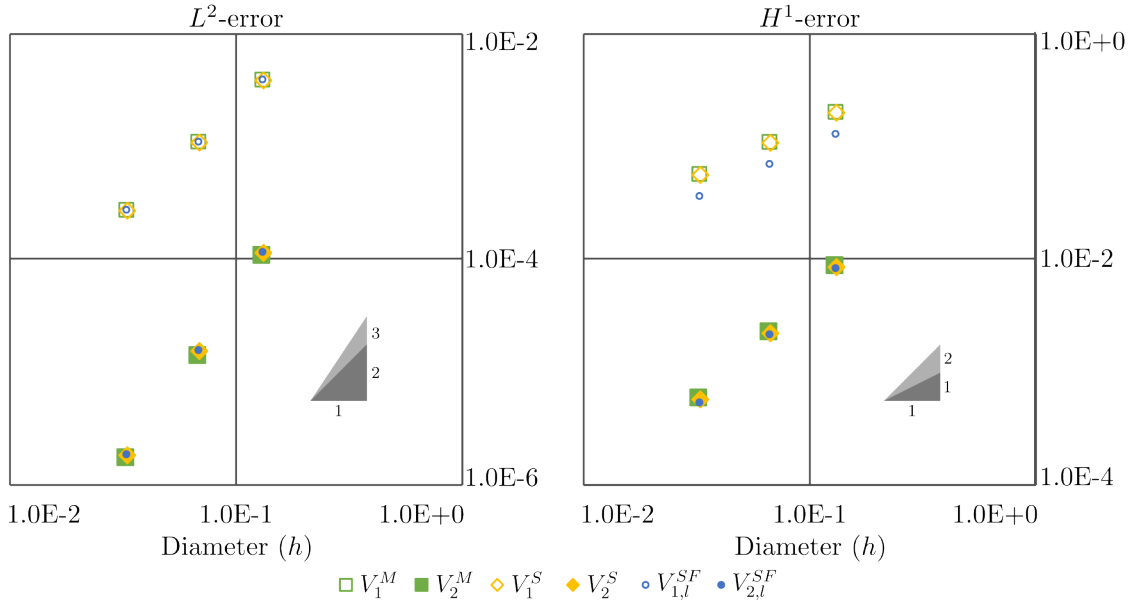

Figure 4. Convergence curves for L^2-error and H^1-error.

thorship of this work, and that all material that has been herein included as part of the present paper is either the property (and authorship) of the authors, or has the permission of the owners to be included here.

References

[1] L. Beirão da Veiga, F. Brezzi, A. Cangiani, G. Manzini, L. D. Marini, and A. Russo. Basic Principles of Virtual Element Methods. *Mathematical Models and Methods in Applied Sciences*, vol. 23, n. 01, pp. 199–214, 2013.

[2] da L. B. Veiga and G. Manzini. A virtual element method with arbitrary regularity. *IMA Journal of Numerical Analysis*, vol. 34, pp. 759–781, 2014.

[3] da L. B. Veiga, F. Brezzi, L. D. Marini, and A. Russo. H(div) and h(curl) -conforming virtual element methods. *Numerische Mathematik*, vol. 133, pp. 303–332, 2016a.

[4] F. Brezzi, R. S. Falk, and L. D. Marini. Basic principles of mixed virtual element methods. *ESAIM: Mathematical Modelling and Numerical Analysis*, vol. 48, pp. 1227–1240, 2014.

[5] H. Chi, A. Pereira, I. F. M. Menezes, and G. H. Paulino. Virtual element method (vem)-based topology optimization: an integrated framework. *Structural and Multidisciplinary Optimization*, vol. 62, pp. 1089–1114, 2020.

[6] da L. B. Veiga, F. Dassi, G. Manzini, and L. Mascotto. Virtual elements for maxwell's equations. *Computers & Mathematics with Applications*, vol. 116, pp. 82–99, 2022.

[7] P. G. Ciarlet. *The finite element method for elliptic problems*. Classics in applied mathematics. Society for Industrial and Applied Mathematics, Great Britain, 2002.

[8] da L. B. Veiga, F. Brezzi, L. D. Marini, and A. Russo. The hitchhiker's guide to the virtual element method. *Mathematical Models and Methods in Applied Sciences*, vol. 24, pp. 1541–1573, 2014.

[9] B. Ahmad, A. Alsaedi, F. Brezzi, L. D. Marini, and A. Russo. Equivalent projectors for virtual element methods. *Computers and Mathematics with Applications*, vol. 66, pp. 376–391, 2013.

[10] da L. B. Veiga, F. Brezzi, L. D. Marini, and A. Russo. Virtual element method for general second-order elliptic problems on polygonal meshes. *Mathematical Models and Methods in Applied Sciences*, vol. 26, pp. 729–750, 2016b.

[11] da L. B. Veiga, F. Brezzi, L. D. Marini, and A. Russo. Serendipity nodal vem spaces. *Computers and Fluids*, vol. 141, pp. 2–12, 2016c.

[12] A. Chen and N. Sukumar. Stabilization-free serendipity virtual element method for plane elasticity. *Computer Methods in Applied Mechanics and Engineering*, vol. 404, pp. 115784, 2023.

[13] A. D'Altri, de S. Miranda, L. Patruno, and E. Sacco. An enhanced vem formulation for plane elasticity. *Computer Methods in Applied Mechanics and Engineering*, vol. 376, pp. 113663, 2021.

[14] B.-B. Xu and P. Wriggers. 3d stabilization-free virtual element method for linear elastic analysis. *Computer Methods in Applied Mechanics and Engineering*, vol. 421, pp. 116826, 2024.